Radboud Universiteit

Structural commensurability and incommensurability in twisted Van der Waals systems

Mikhail Katsnelson

IMM
Institute for Molecules and Materials

Grisha Volovik and the unity of physics

My small experience

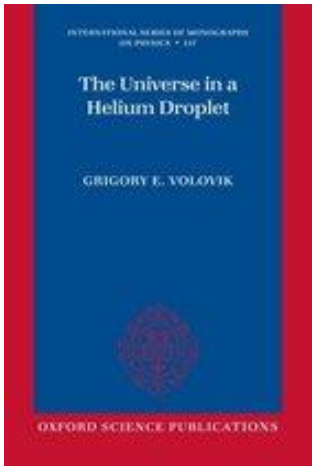

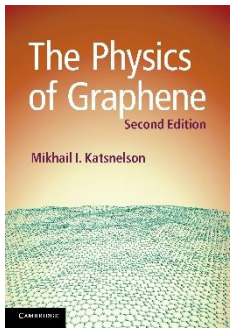

ISSN 0021-3640, JETP Letters, 2012, Vol. 95, No. 8, pp. 411–415. © Pleiades Publishing, Inc., 2012.

Quantum Electrodynamics with Anisotropic Scaling: Heisenberg–Euler Action and Schwinger Pair Production in the Bilayer Graphene¶

M. I. Katsnelson[a] and G. E. Volovik[b, c]

[a] Radboud University Nijmegen, Institute for Molecules and Materials, NL-6525AJ Nijmegen, The Netherlands
[b] Low Temperature Laboratory, Aalto University, School of Science and Technology, P.O. Box 15100, FI-00076 AALTO, Finland
[c] Landau Institute for Theoretical Physics, Russian Academy of Sciences, Moscow, 119334 Russia
e-mail: m.katsnelson@science.ru.nl, volovik@boojum.hut.fi

Received March 11, 2012

J Low Temp Phys (2014) 175:655–666
DOI 10.1007/s10909-014-1167-8

Topological Matter: Graphene and Superfluid ^{3}He

M. I. Katsnelson · G. E. Volovik

Abstract The physics of graphene and of the superfluid phases of ^{3}He have many common features. Both systems are topological materials where quasiparticles behave as relativistic massless (Weyl, Majorana or Dirac) fermions. We formulate the points where these features are overlapping. This will allow us to use graphene to study the properties of superfluid ^{3}He, to use superfluid ^{3}He to study the properties of graphene, and to use both of them in combination to study the physics of topological quantum vacuum. We suggest also some particular experiments with superfluid ^{3}He using graphene as an atomically thin membrane impenetrable for He atoms but allowing for spin, momentum and energy transfer.

Annals of Physics 331 (2013) 160–187

Contents lists available at SciVerse ScienceDirect

Annals of Physics

journal homepage: www.elsevier.com/locate/aop

Euler–Heisenberg effective action and magnetoelectric effect in multilayer graphene

M.I. Katsnelson[a,*], G.E. Volovik[b,c], M.A. Zubkov[d]

[a] Radboud University Nijmegen, Institute for Molecules and Materials, Heyndaalseweg 135, NL-6525AJ Nijmegen, The Netherlands
[b] Low Temperature Laboratory, School of Science and Technology, Aalto University, P.O. Box 15100, FI-00076 AALTO, Finland
[c] L. D. Landau Institute for Theoretical Physics, Kosygina 2, 119334 Moscow, Russia
[d] ITEP, B. Cheremushkinskaya 25, Moscow, 117259, Russia

Annals of Physics 336 (2013) 36–55

Contents lists available at SciVerse ScienceDirect

Annals of Physics

journal homepage: www.elsevier.com/locate/aop

Unruh effect in vacua with anisotropic scaling: Applications to multilayer graphene

M.I. Katsnelson[a], G.E. Volovik[b,c], M.A. Zubkov[d,*]

[a] Radboud University Nijmegen, Institute for Molecules and Materials, Heyndaalseweg 135, NL-6525AJ Nijmegen, The Netherlands
[b] Low Temperature Laboratory, School of Science and Technology, Aalto University, P.O. Box 15100, FI-00076 Aalto, Finland
[c] L. D. Landau Institute for Theoretical Physics, Kosygina 2, 119334 Moscow, Russia
[d] ITEP, B.Cheremushkinskaya 25, Moscow, 117259, Russia

Happy birthday Grisha!

Outline

I. Phase synchronization and commensurate – incommensurate transition in general
II. Graphene on hBN: (1) atomic reconstruction; (2) effect on electronic structure; (3) transport; (4) nonlinear optics
III. Graphene on graphite and/or twisted bilayer graphene: (1) atomic reconstruction and vortex lattice formation; (2) description in terms of misfit dislocations; (3) pseudomagnetic field and electronic structure
IV. Many-body effects at Van Hove filling in 2D systems: flat band formation

Example: Graphene on hBN

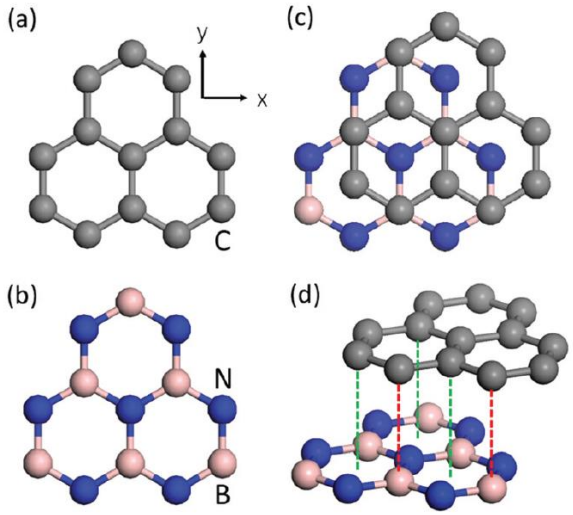

Chen & Qin, JPCC 8, 12085 (2020)

Graphene and hexagonal boron nitride (hBN) have the same crystal structure but slightly different interatomic distances (roughly, 0.142 nm vs 0.145 nm). In hBN they are 1.8% larger

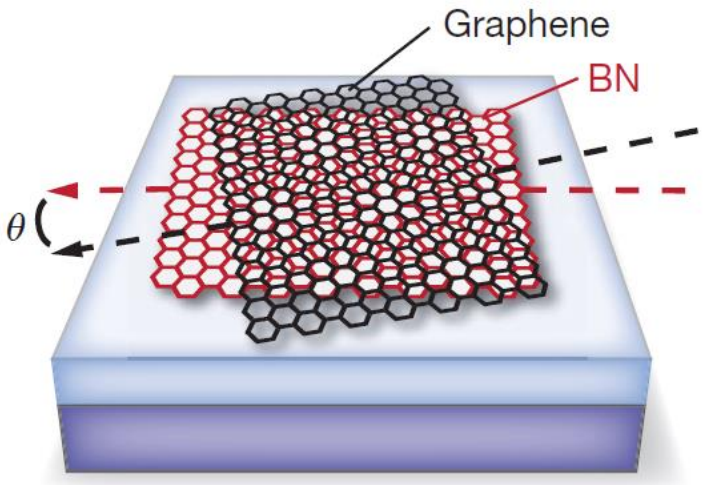

Dean et al, Nature 497, 598 (2013)

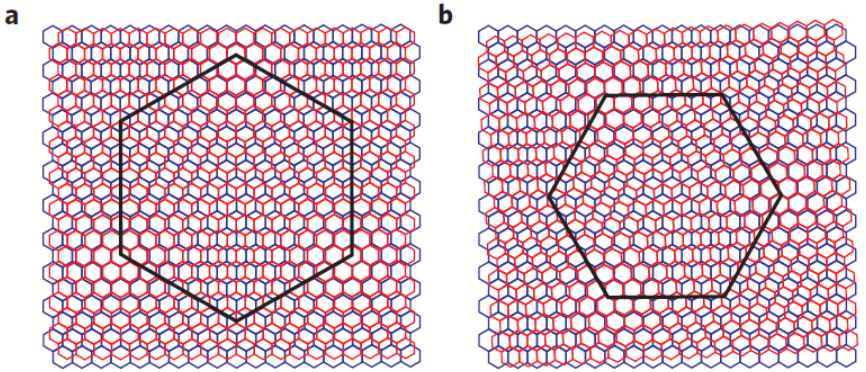

Figure 1 | Schematic representation of the moiré pattern of graphene (red) on hBN (blue). a Relative rotation angle between the crystals $\varphi = 0°$. **b** Relative rotation angle between the crystals $\varphi = 3° \approx 0.052$ rad. The mismatch between the lattices is exaggerated (~10%). Black hexagons mark the moiré plaquette.

Woods et al, Nature Phys. 10, 451 (2014)

Phase locking (synchronization)

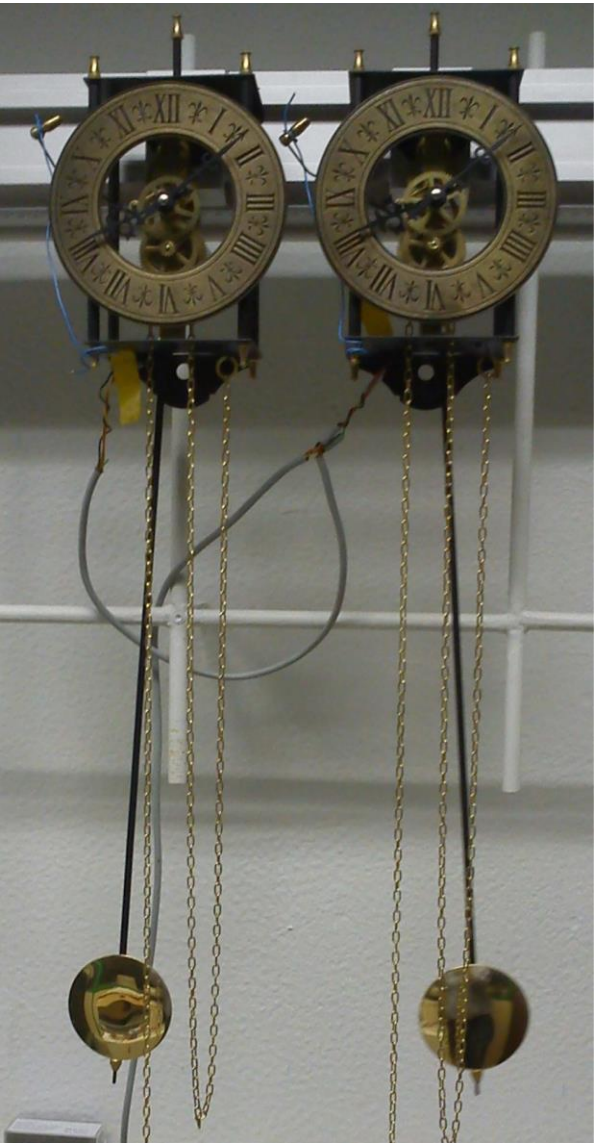

Oliveira & Melo, Sci Rep 2015

Discovered by Huygens, XVII century)

If you have two coupled oscillators with slightly different frequencies they can be synchronized

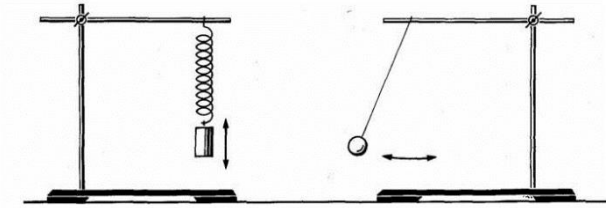

E.g., string pendulum, frequency ratio close to 1:2

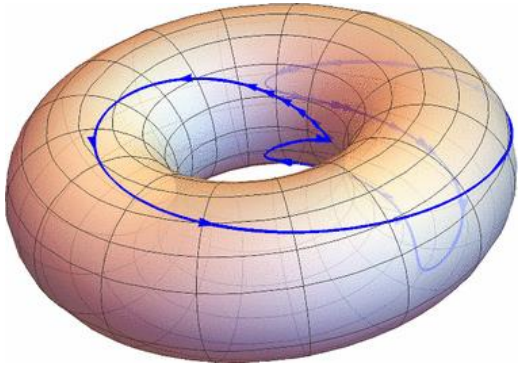

Llibre et al, J. Dyn. Dif. Eq. (2018)

Bifurcation of torus (with two incommensurate frequencies) into limit circle (with one common period)

Misfit dislocations

One-dimensional dislocations.
I. Static theory

By F. C. Frank and J. H. van der Merwe
H. H. Wills Physical Laboratory, University of Bristol

(*Communicated by N. F. Mott, F.R.S.—Received 22 December 1948—Revised 25 March 1949—Read 19 May 1949*)

$$V_N = \tfrac{1}{2}\mu \sum_{n=0}^{N-1} (x_{n+1} - x_n + a - b)^2 + \tfrac{1}{2}W \sum_{n=0}^{N-1} (1 - \cos 2\pi x_n/a)$$

Energy of interlayer interaction (second term) wants that interatomic distances are equal but then one pays for the energy of elastic deformation (the first term)

Interface of different semiconductors (e.g. PbTe/PbSe)

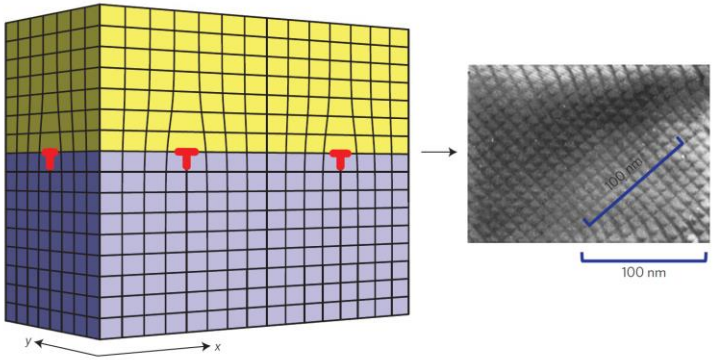

Tang & Fu, Nature Phys. 10, 964 (2014)

Very roughly: When $W > \mu(b-a)^2$ then two layers will be mostly commensurate, and the whole misfit will be concentrated via narrow 'solitons', and in the opposite limit the system will not even try To reach synchronization of periods, that is, commensurability

Commensurate – incommensurate transition is expected!

Commensurate-incommensurate transition

Commensurate–incommensurate transition in graphene on hexagonal boron nitride

C. R. Woods[1], L. Britnell[1], A. Eckmann[2], R. S. Ma[3], J. C. Lu[3], H. M. Guo[3], X. Lin[3], G. L. Yu[1], Y. Cao[4], R. V. Gorbachev[4], A. V. Kretinin[1], J. Park[1,5], L. A. Ponomarenko[1], M. I. Katsnelson[6], Yu. N. Gornostyrev[7], K. Watanabe[8], T. Taniguchi[8], C. Casiraghi[2], H-J. Gao[3], A. K. Geim[4] and K. S. Novoselov[1]*

NATURE PHYSICS DOI: 10.1038/NPHYS2954

When misorientation angle (in radians) is smaller with misfit, synchronization happens

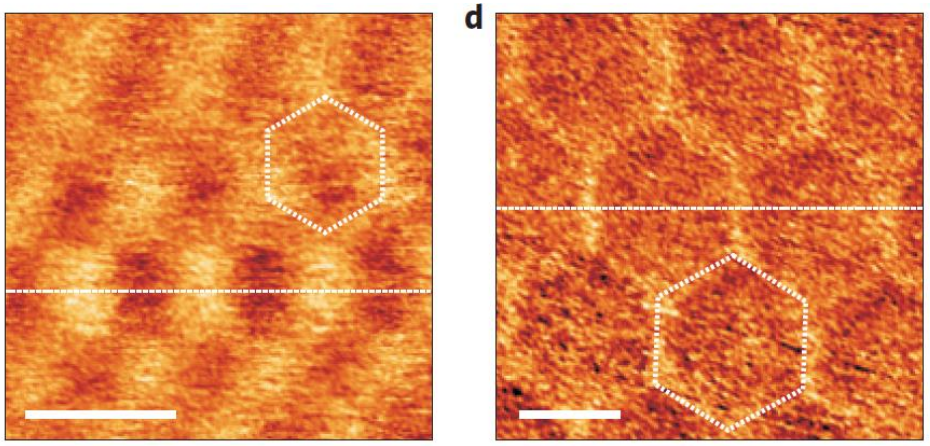

Moire patterns with periodicity 8 nm (left) and 14 nm (right)

Atomistic simulations

PRL 113, 135504 (2014) PHYSICAL REVIEW LETTERS week ending 26 SEPTEMBER 2014

Moiré Patterns as a Probe of Interplanar Interactions for Graphene on h-BN

M. M. van Wijk, A. Schuring, M. I. Katsnelson, and A. Fasolino*

Distribution of bond length in commensurate (left) and incommensurate (right) regimes

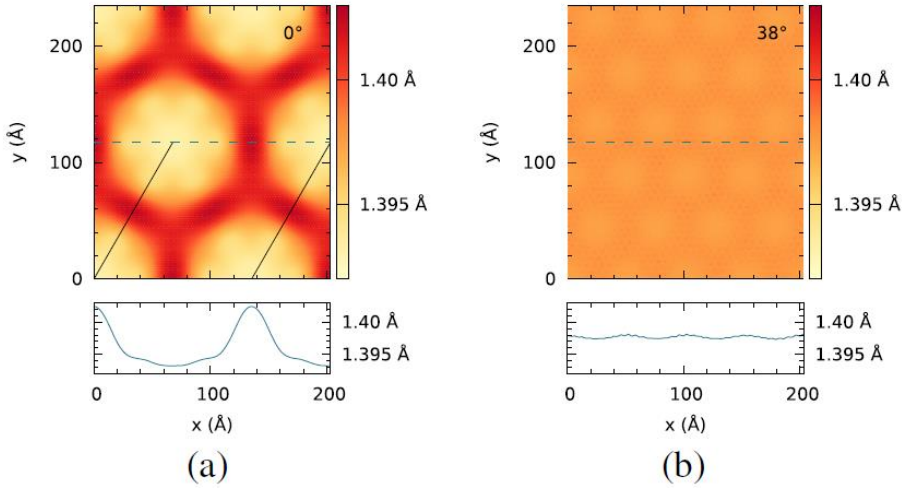

Consequences for electronic structure

PHYSICAL REVIEW B **84**, 195414 (2011)

Adhesion and electronic structure of graphene on hexagonal boron nitride substrates

B. Sachs,[1,*] T. O. Wehling,[1,†] M. I. Katsnelson,[2] and A. I. Lichtenstein[1]

Relaxed structure (B green, C yellow, N red)

V corresponds to the minimal energy (max. cohesion)

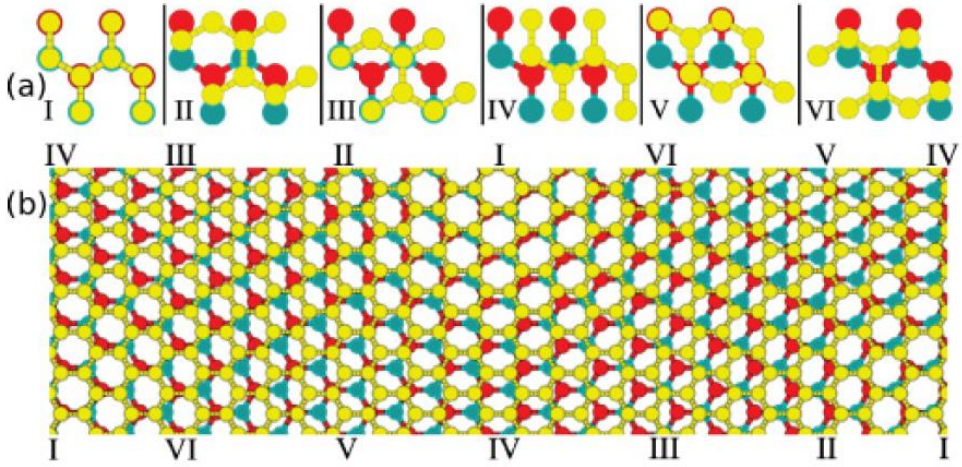

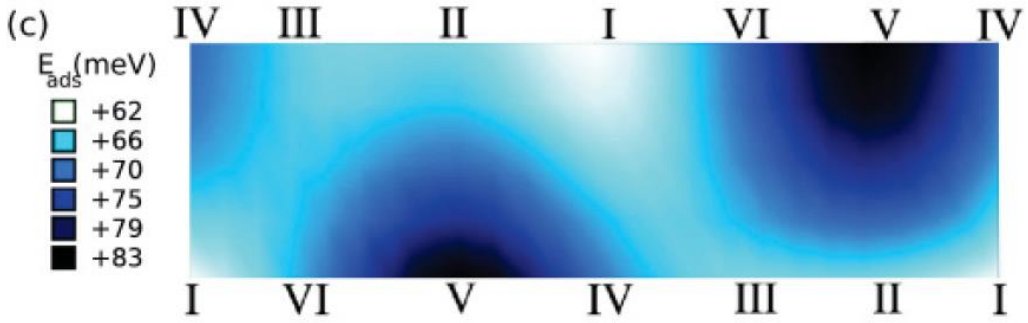

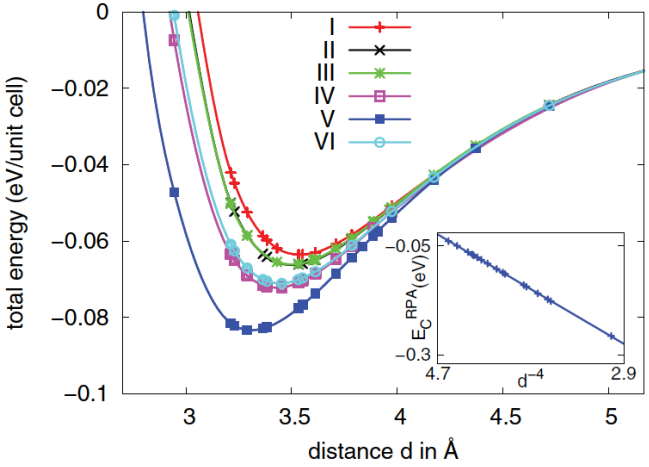

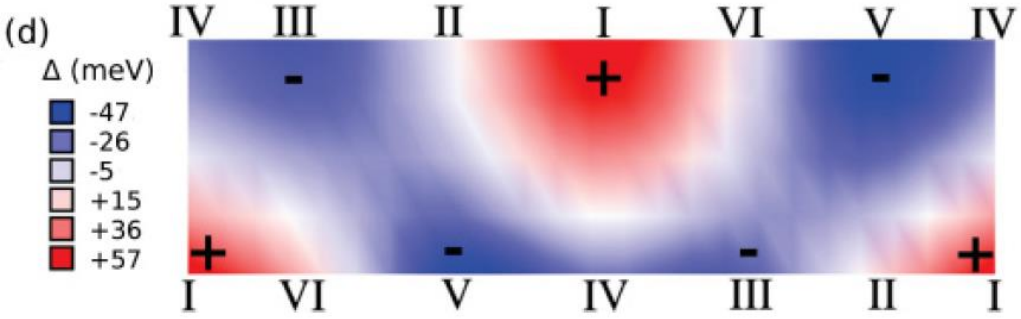

B on the top of C, N in the middle of hexagon
Sublattices are no more equivalent → locally energy gap is open (mass term in Dirac eq.)

Consequences for electronic structure II

PRL 115, 186801 (2015) PHYSICAL REVIEW LETTERS week ending 30 OCTOBER 2015

Effect of Structural Relaxation on the Electronic Structure of Graphene on Hexagonal Boron Nitride

G. J. Slotman,[1] M. M. van Wijk,[1] Pei-Liang Zhao,[2] A. Fasolino,[1] M. I. Katsnelson,[1] and Shengjun Yuan[1,*]

Atomic relaxation in commensurate phase modulates the Hamiltonian parameters

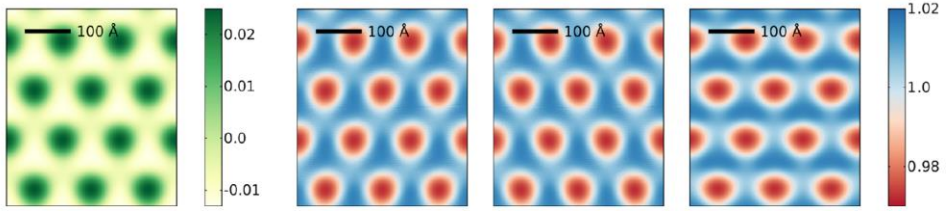

FIG. 1 (color online). The modified TB parameters for a relaxed sample of graphene on hBN with $\theta = 0°$ ($\lambda = 13.8$ nm). From left to right, the on-site potential v and the hopping parameters t_1, t_2, and t_3. The color bars are in units of $t = 2.7$ eV.

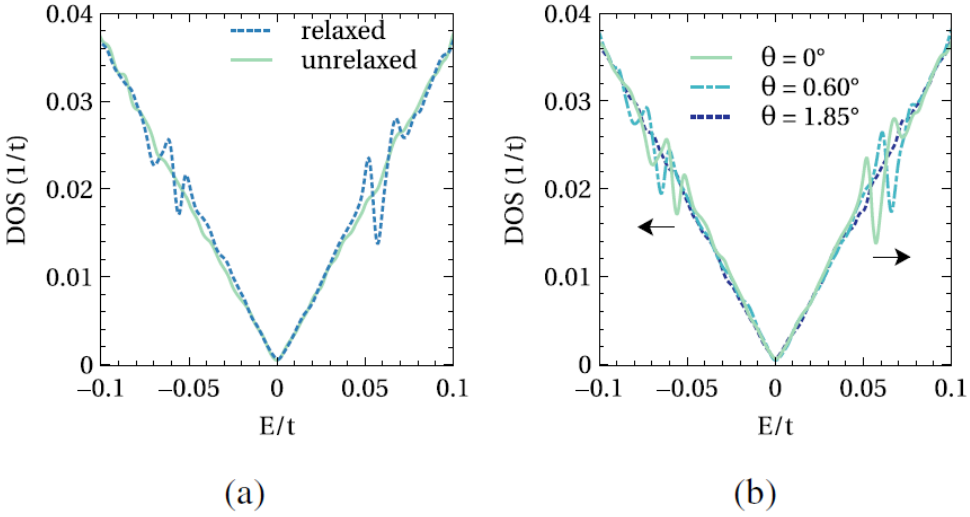

Very strong effect of atomic relaxation!

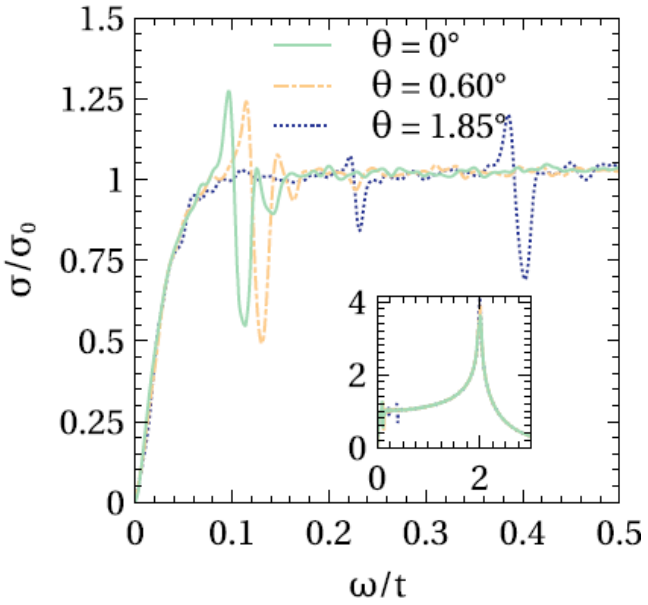

Optical conductivity

Consequences for electronic transport

In commensurate phase average gap is non zero, and system can be insulating

For incommensurate phase, the average gap is zero, and there are electron states along zero-mass lines (Tudorovskiy & MIK, PRB **86**, 045419 (2012)

Model of percolation along zero-mass lines

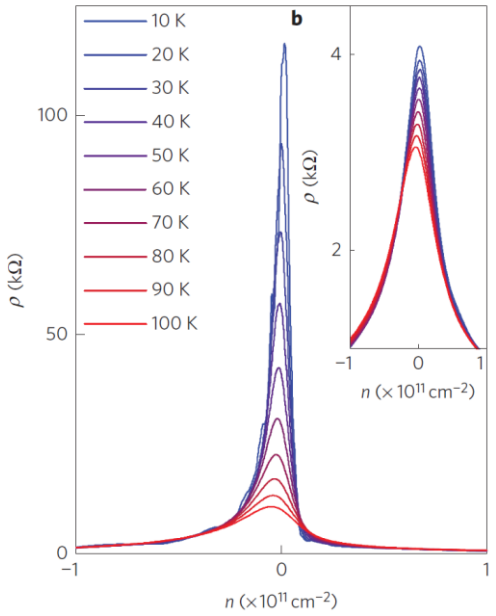

Woods et al, Nature Phys. 10, 451 (2014)

PRL 113, 096801 (2014) PHYSICAL REVIEW LETTERS week ending 29 AUGUST 2014

Metal-Insulator Transition in Graphene on Boron Nitride

M. Titov and M. I. Katsnelson

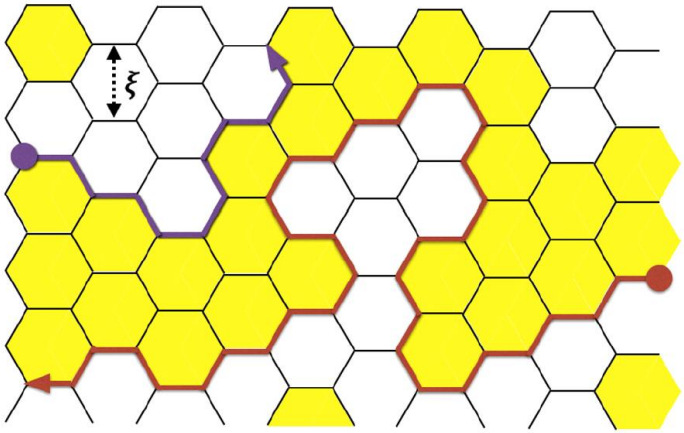

Landauer formula $G = \frac{2e^2}{h}\langle N_{line}\rangle$

Exact result for 2D percolation (Cardy) $\langle N_{line}\rangle = \frac{\sqrt{3}}{2}\frac{L_x}{L_y}$

Exact minimal conductivity in percolation model $\sigma = \sqrt{3}\frac{e^2}{h}$

Optical second-harmonic generation

In commensurate phase inversion symmetry in broken due to nonequivalence of sublattices → second-harmonic generation (SHG) is allowed by symmetry

PHYSICAL REVIEW B **99**, 165432 (2019)

Resonant optical second harmonic generation in graphene-based heterostructures

M. Vandelli,[1,2] M. I. Katsnelson,[1,3] and E. A. Stepanov[1,3]

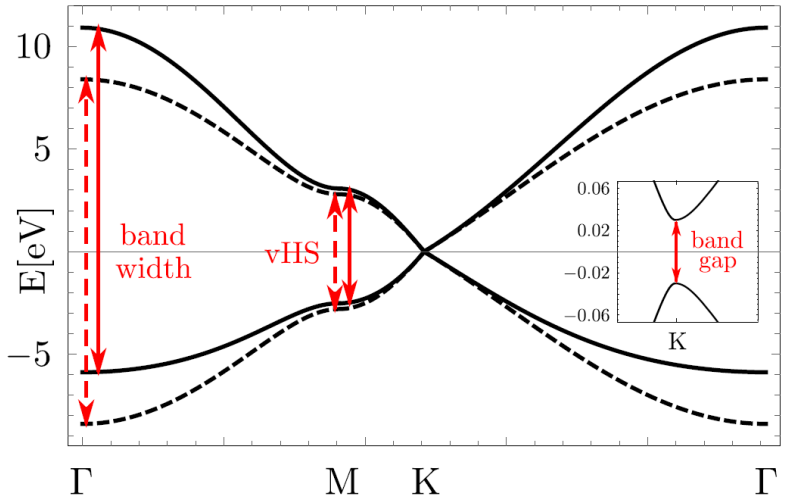

FIG. 1. Dispersion relation of graphene with (solid line) and without (dashed line) account for the next-nearest-neighbor hopping process t'. Red arrows show optical resonances at the bandwidth (Γ point), van Hove singularity (M point), and band gap (K point).

$t = -2.8$ eV, $t' = -0.1t$ $m = 30$ meV

Electron-hole symmetry should be also broken → either final doping or NNN hopping t'

$$\hat{H}_{ij}[A] = \hat{H}_{ij} \exp\left(-i\frac{e}{c}\int_{\mathbf{R}_i}^{\mathbf{R}_j} \mathbf{A}(\mathbf{r},t)\cdot d\mathbf{r}\right)$$

Contributions to nonlinear optical conductivity

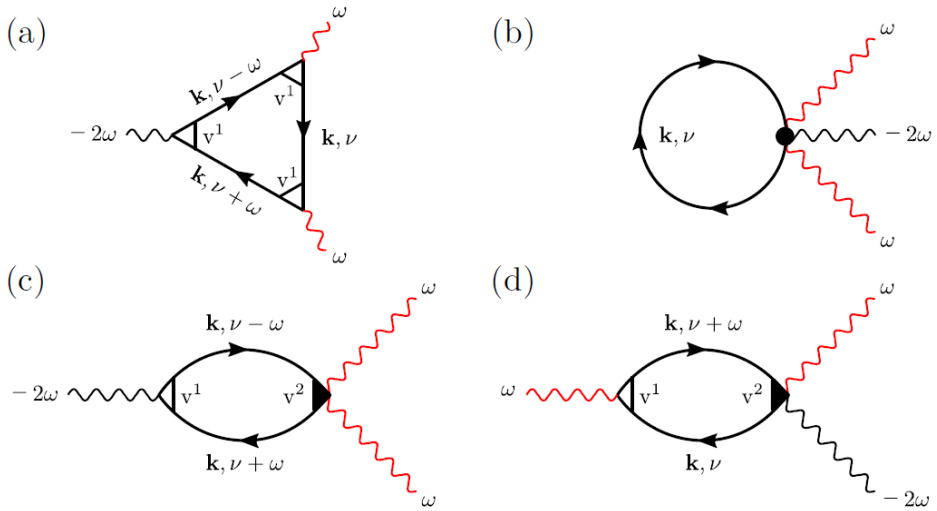

Optical SHG II

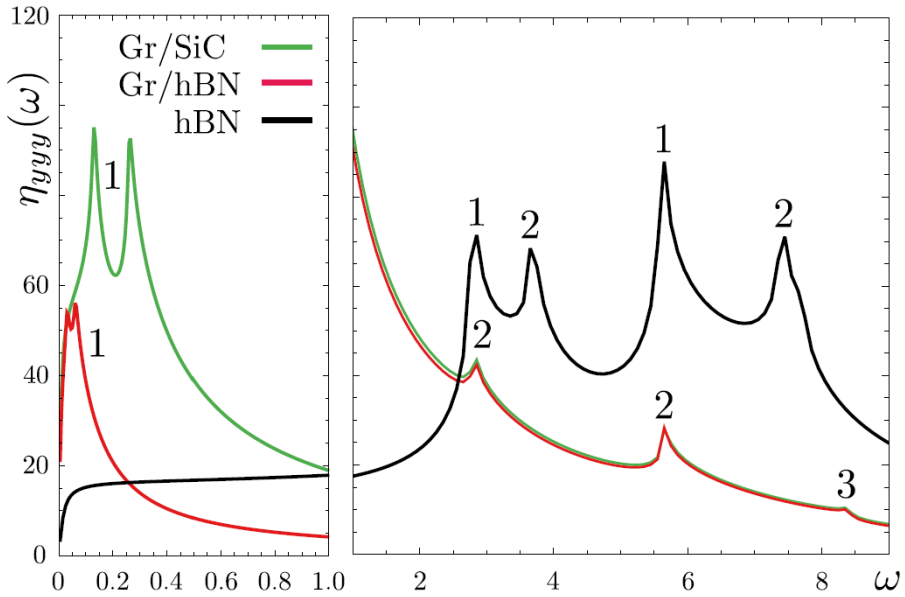

FIG. 3. The absolute value of $\eta_{yyy}(\omega)$ for hBN (black line), Gr/SiC (green line), and Gr/hBN (red line) at low (left) and high (right) frequency ω. The data for Gr/SiC on the right panel is multiplied by a factor of 5 and data for Gr/hBN is multiplied by $5 \times (m_{\mathrm{Gr/SiC}}/m_{\mathrm{Gr/hBN}})$. The data on the left panel is shown without the multiplication. Labels "1," "2," and "3" depict resonances on the band gap, van Hove singularity, and the bandwidth, respectively. The frequency ω of the applied light is given in units of eV.

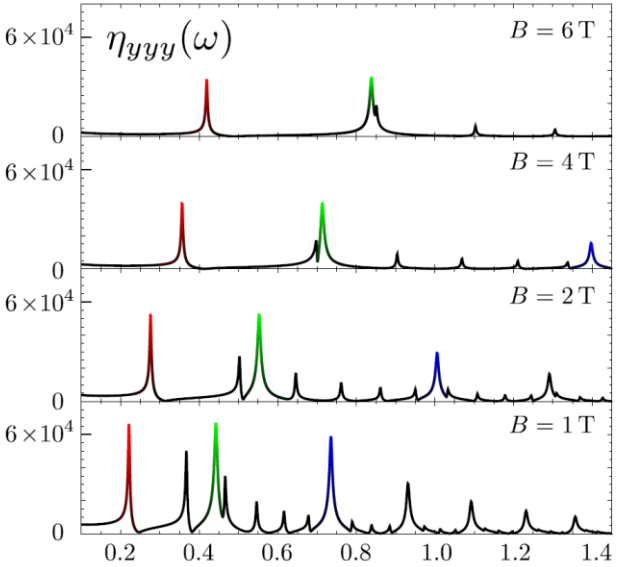

FIG. 5. The absolute value of $\eta_{yyy}(\omega)$ (in a.u.) as the function of the frequency of the applied light ω (in eV) for the case of Gr/SiC under the effect of the magnetic field $B = 1$ T, 2 T, 4 T, and 6 T. Colors serve as guides to the eye and depict resonances on the same Landau levels at different values of the magnetic field.

Optical SHG III

Direct Observation of Incommensurate–Commensurate Transition in Graphene-hBN Heterostructures via Optical Second Harmonic Generation

E. A. Stepanov,*,† S. V. Semin,† C. R. Woods, M. Vandelli, A. V. Kimel, K. S. Novoselov, and M. I. Katsnelson

Cite This: *ACS Appl. Mater. Interfaces* 2020, 12, 27758–27764 Read Online

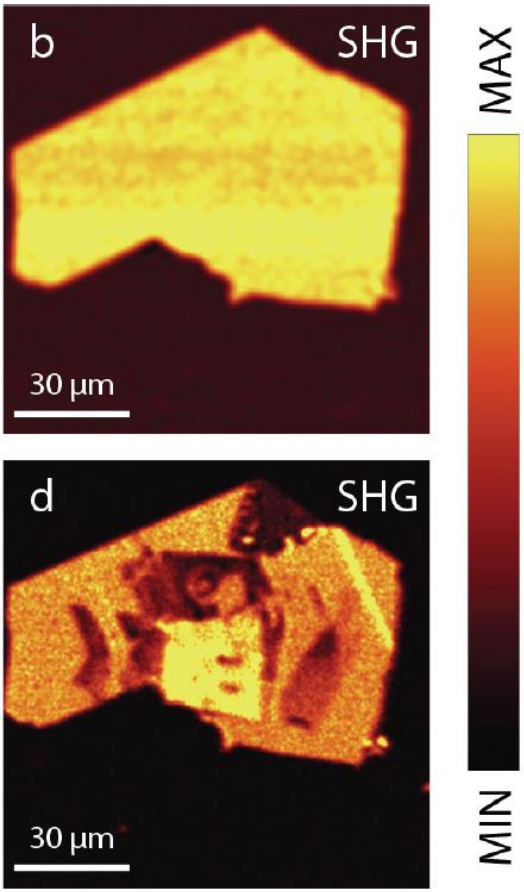

b – incommensurate phase, only hBN signal is visible;
d – commensurate, one can see graphene

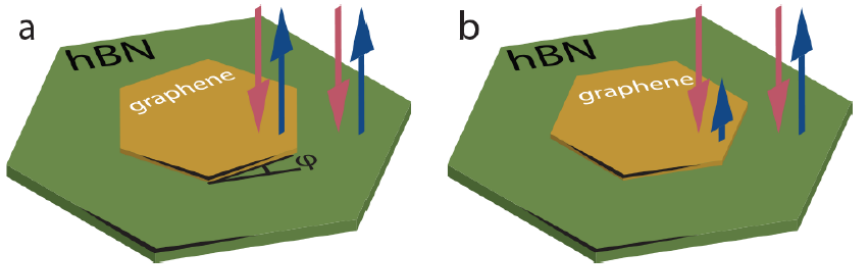

Figure 1. Sketch of the experiment. Green and yellow hexagonal tiles represent hBN and graphene, respectively. Red arrows depict the incident 800 nm light. Blue arrows indicate the SHG response collected at 400 nm from different parts of the sample. (a) In the incommensurate phase, the inversion symmetry of graphene is not broken, and the uniform signal of the SHG comes only from the hBN. (b) After the structural phase transition to the commensurate state, strong modification of the SHG response is observed from the graphene area, where the inversion symmetry breaking is induced by the aligned hBN substrate.

Commensurate – incommensurate transition was induced by ieating and clearly detected via SHG

Graphene on graphite

Relaxation of moiré patterns for slightly misaligned identical lattices: graphene on graphite

2D Mater. **2** (2015) 034010

M M van Wijk, A Schuring, M I Katsnelson and A Fasolino

Atomistic simulations: graphene on graphite

Periodicity of moire structure $a_m = \dfrac{a_{\text{lattice}}}{2|\sin(\theta/2)|}$

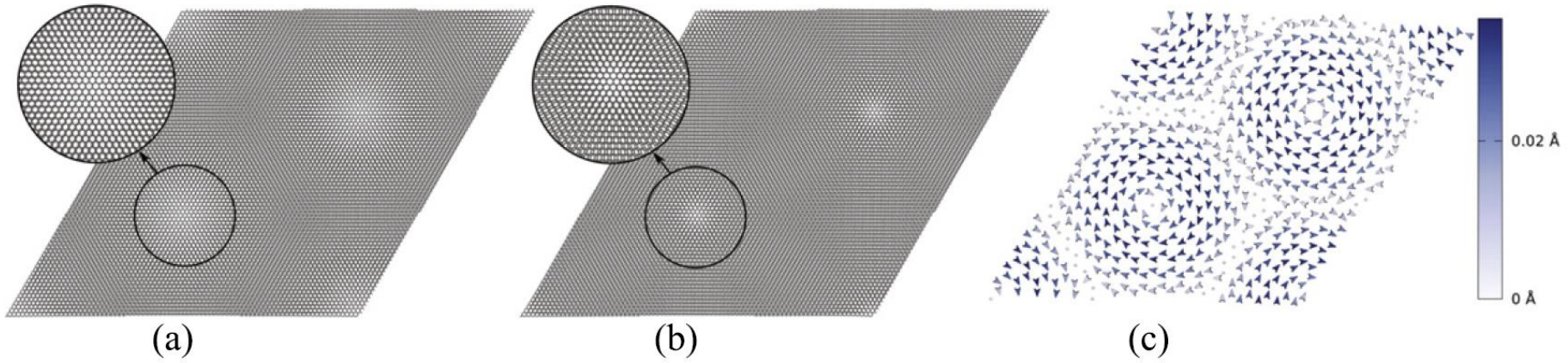

Figure 2. The effects of relaxation are shown for a sample with $(n, m) = (82,1)$, $\theta = 1.2°$ and $a_m = 115.3$ Å. (a) The sample prior to relaxation, (b) the sample after relaxation. Notice the shrinking of the AA stacked area. (c) The displacements of the atoms as the result of relaxation for a sample $(n, m) = (17,1)$, $\theta = 5.7°$ and $a_m = 24.5$ Å. The colour indicates size and the arrow the direction of the displacements.

Graphene on graphite II

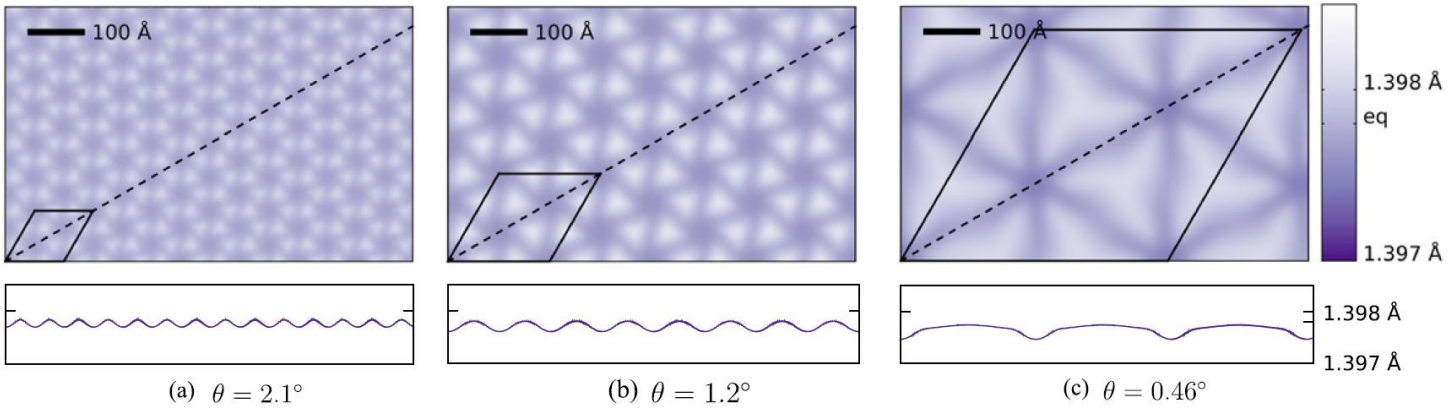

Figure 4. Bond lengths of relaxed configurations for samples where the graphene layer is relaxed in all directions. The supercell is shown in black. The bottom panels show the bond length along the dashed diagonal line. (a) $\theta = 2.1°$, $(n, m) = (47,1)$, $a_m = 66.4$ Å. (b) $\theta = 1.2°$, $(n, m) = (82,1)$, $a_m = 115.3$ Å. (c) θ=0.46°, $(n, m) = (216,1)$, $a_m = 302.6$ Å.

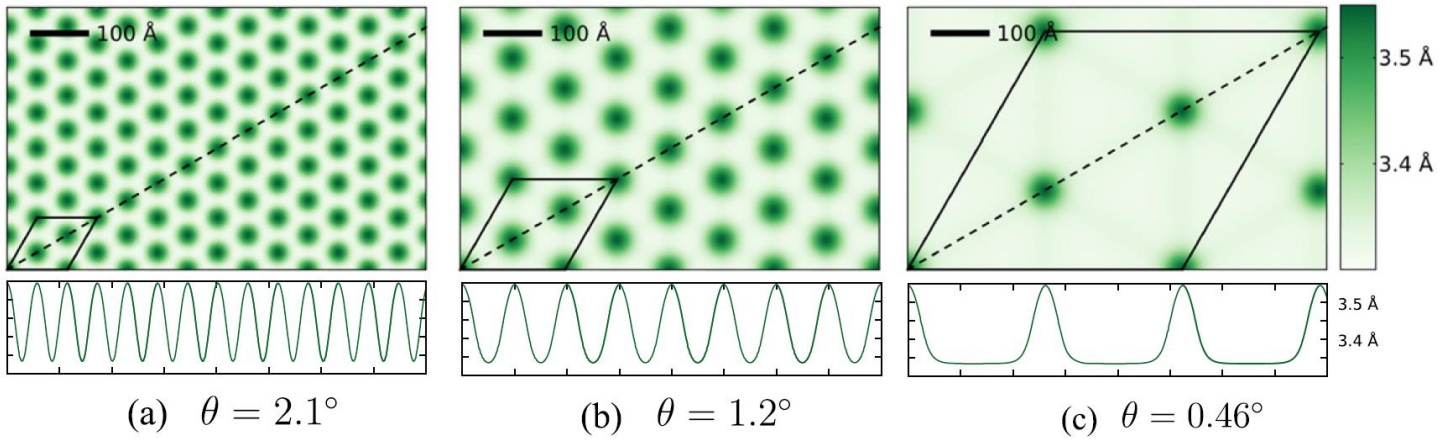

Figure 6. Out-of-plane distance for samples where the graphene layer is relaxed in all dimensions. The bottom panels show the out-of-plane distance along the dashed diagonal line. (a) $\theta = 2.1°$, $(n, m) = (47,1)$, $a_m = 66.4$ Å. (b) $\theta = 1.2°$, $(n, m) = (82,1)$, $a_m = 115.3$ Å. (c) $\theta = 0.46°$, $(n, m) = (216,1)$, $a_m = 302.6$ Å.

Twisted bilayer graphene

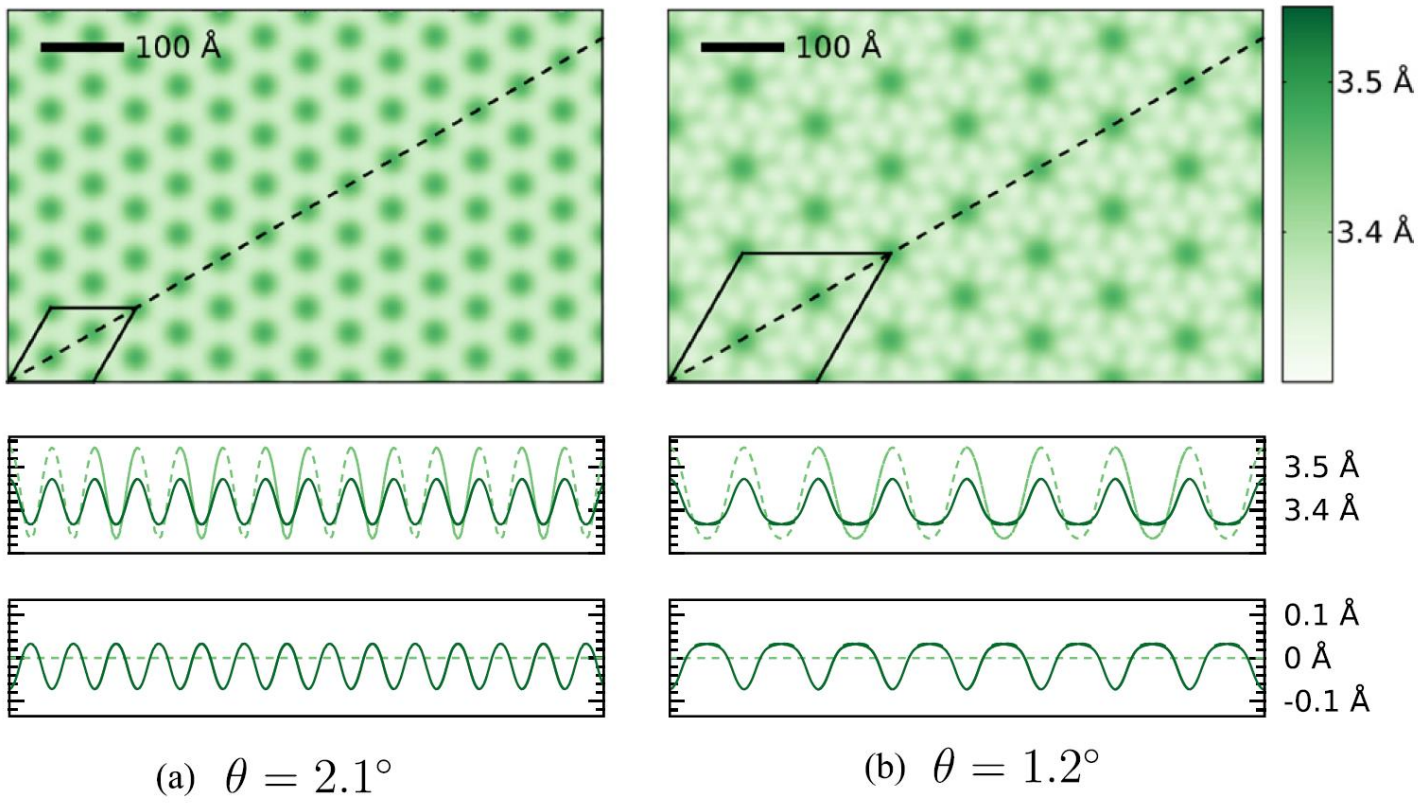

Figure 8. Out-of-plane distance for double layer graphene. The bottom four panels show z along the dashed line in the top figure. The dashed lines show the z for graphene on graphite as in figure 6.

There is a modulation at small angles and some analog of "incommensurability" (small modulations) at larger angles

Description in terms of dislocations

PHYSICAL REVIEW B **102**, 085428 (2020)

Origin of the vortex displacement field in twisted bilayer graphene

Yu. N. Gornostyrev [1,2] and M. I. Katsnelson [3,2]

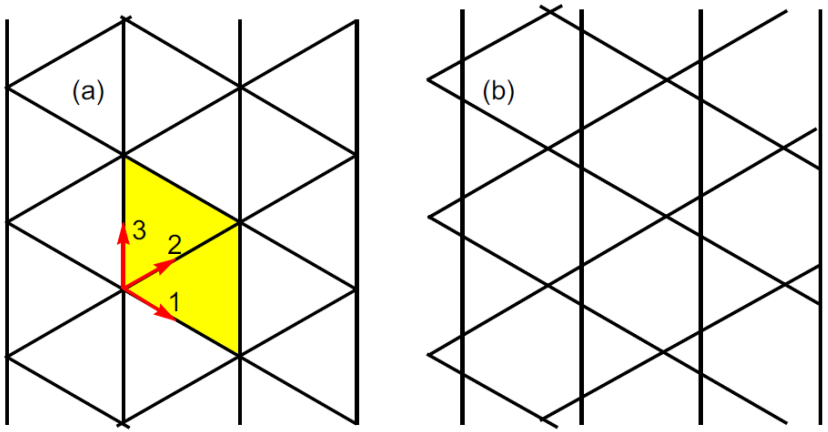

FIG. 1. The schematic representation of the dislocation network used to describe the twist boundary. (a) Network of screw dislocations. (b) Reconstructed network of dislocations. Vectors 1–3 indicate the directions of dislocation lines. The moiré cell is highlighted by a yellow tetragon.

To reproduce vortex structure one can try three families of screw dislocations

Displacement field from individual dislocation is given by analytic formula (Frenkel – Kontorova model)

$$u_s(x) = \frac{b}{\pi}\sum_i \left\{\arctan\left[\exp\left(\frac{x - x_i^0 - \delta/2}{\xi}\right)\right] + \arctan\left[\exp\left(\frac{x - x_i^0 + \delta/2}{\xi}\right)\right]\right\},$$

δ dislocation core splitting

$\delta \sim \mu b/\gamma$ μ is the shear modulus

γ is the stacking fault energy

Description in terms of dislocations II

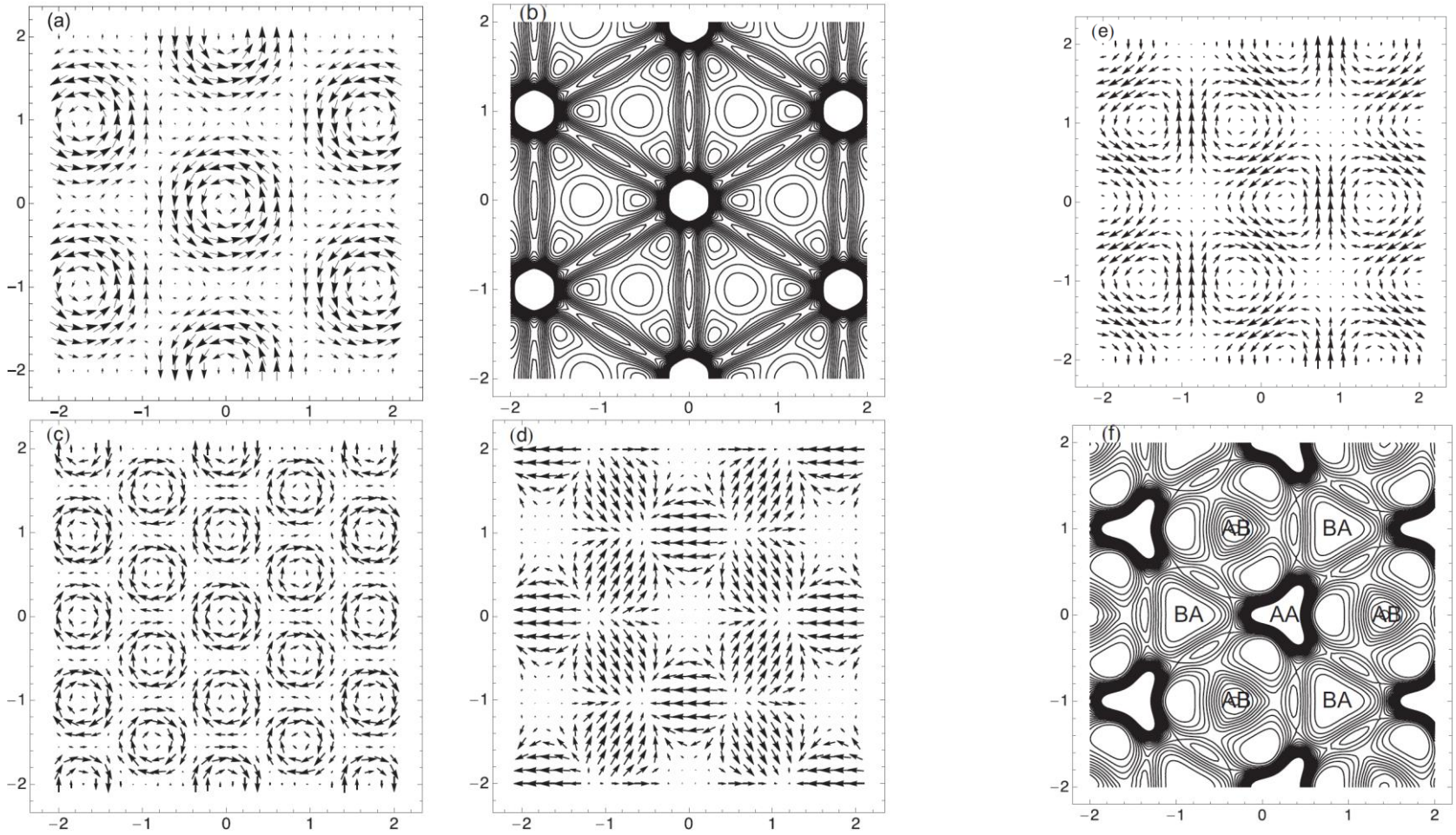

FIG. 3. Displacement $\mathbf{u}_{el}(\mathbf{r})$ shown as a vector field for (a) narrow and (c), (d) split dislocation cores ($\delta = 0.4d$), and (e) for the reconstructed dislocation network. (c) and (d) display screw and edge components of the displacement field, respectively, in the case of split dislocation. (b) and (f) present the distribution of the strain energy density determined by Eq. (9) for cases (a) and (e), respectively. The value ξ is equal $0.05d$ in cases (a)–(c) and $0.15d$ in cases (e) and (f). Distances along the X, Y axes are given in units of $L\sqrt{3}/2$, where L is the separation between the moiré coincidence points.

Description in terms of dislocations III

Pseudomagnetic fields

$$A_x = -2c\beta t u_{xy}.$$

$$A_y = -c\beta t\left(u_{xx} - u_{yy}\right)$$

$$\frac{evB}{c} = \frac{\partial A_y}{\partial x} - \frac{\partial A_x}{\partial y}$$

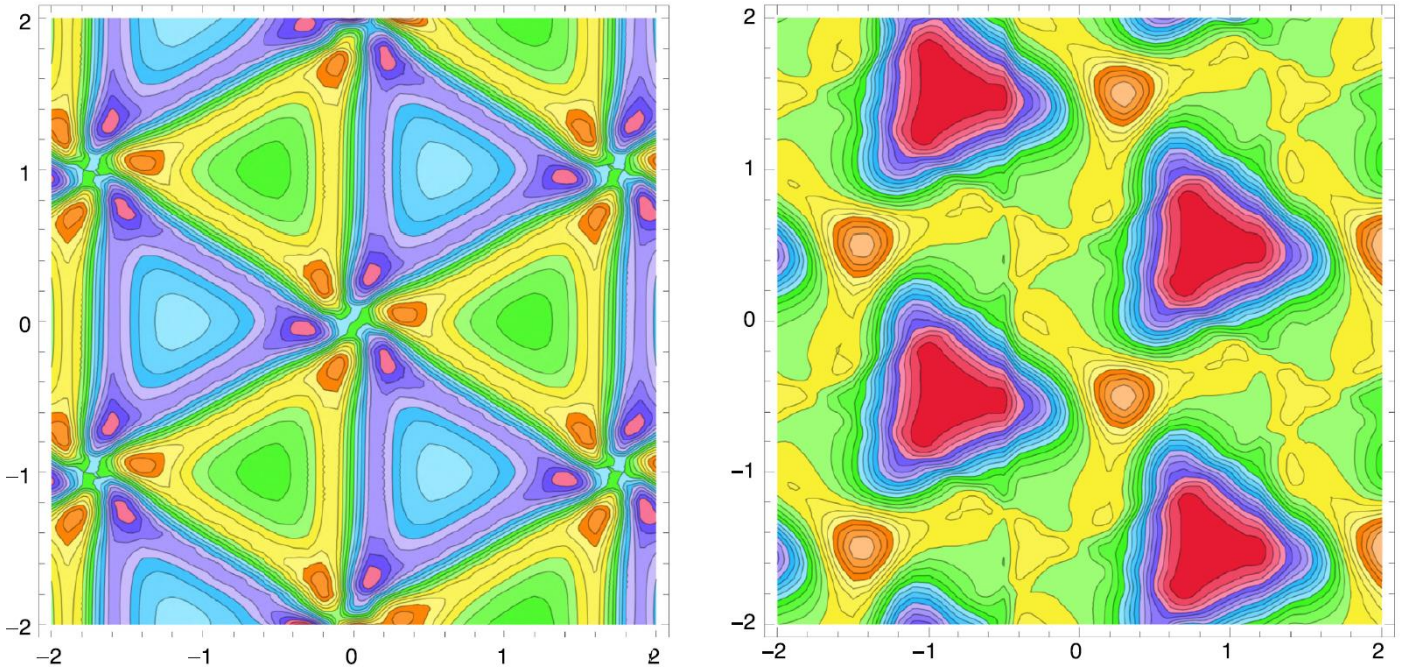

FIG. 5. Distribution of PMF calculated by using Eqs. (10) and (11) for the network of narrow dislocations shown in Fig. 3(a) (left) and for the reconstructed dislocation network shown in Fig. 3(e) (right). Distances along the X, Y axes are given in units of $L\sqrt{3}/2$, where L is the separation between the moiré coincidence points.

There is an analytic formula for pseudomagnetic field, quite cumbersome but explicit

Description in terms of vortices is consistent with that in terms of dislocations

For graphene at hBN one needs to add three families of edge dislocations, due to lattice misfit

Large-scale TB simulations plus experiment

Large-area, periodic, and tunable intrinsic pseudo-magnetic fields in low-angle twisted bilayer graphene

NATURE COMMUNICATIONS | (2020)11:371

Haohao Shi[1,2,6], Zhen Zhan[3,6], Zhikai Qi[4], Kaixiang Huang[3], Edo van Veen[5], Jose Ángel Silva-Guillén[3], Runxiao Zhang[1,2], Pengju Li[1,2], Kun Xie[1,2], Hengxing Ji[4], Mikhail I. Katsnelson[5], Shengjun Yuan[3*], Shengyong Qin[1,2*] & Zhenyu Zhang[1]

Atomic relaxation effects are essential

Electronic properties of TBG with twist angle $\theta = 0.48°$

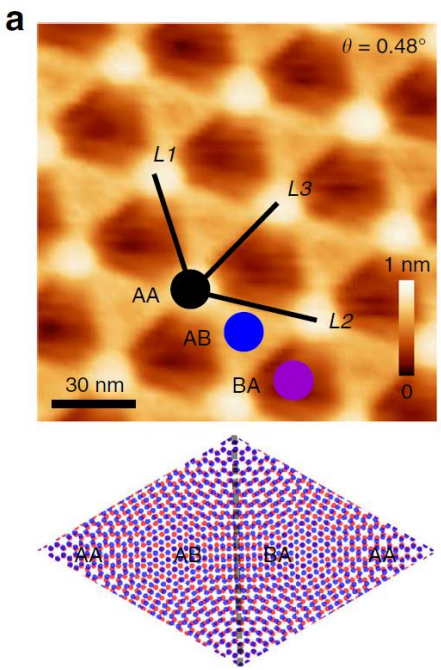

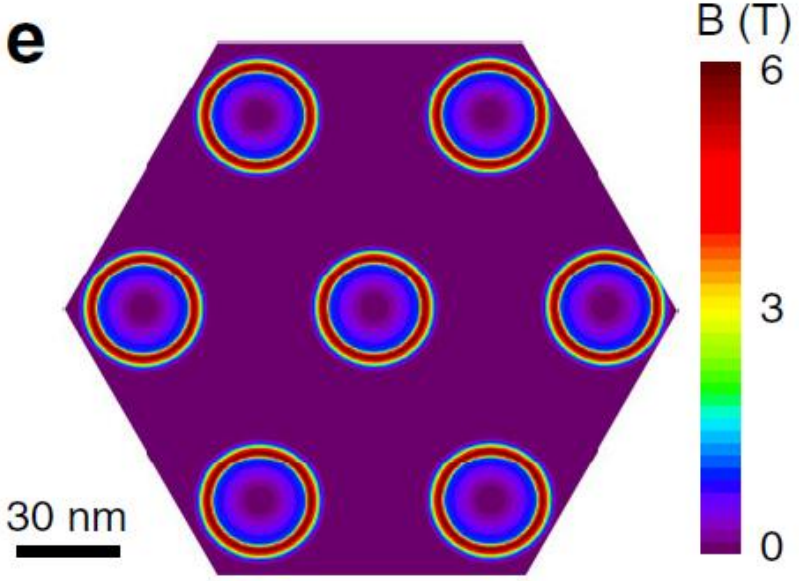

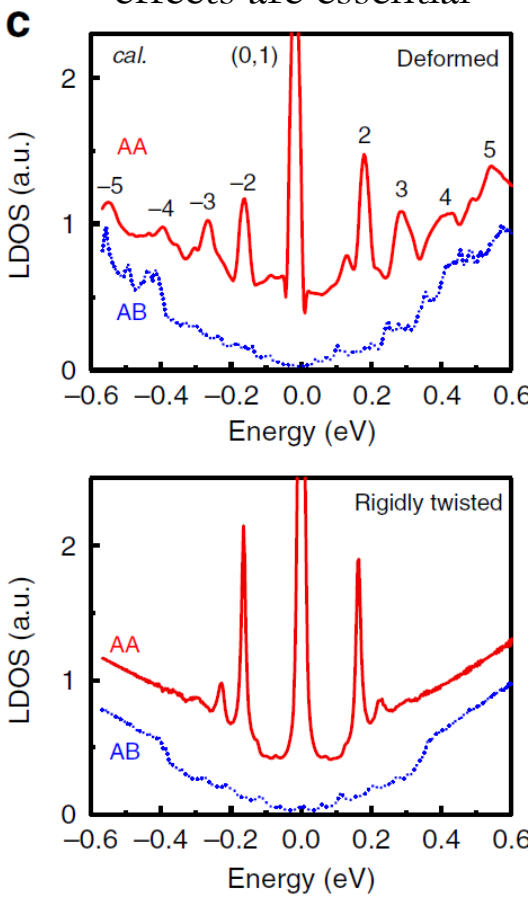

Calculated distribution of pseudomagnetic field

Large-scale TB simulations plus experiment

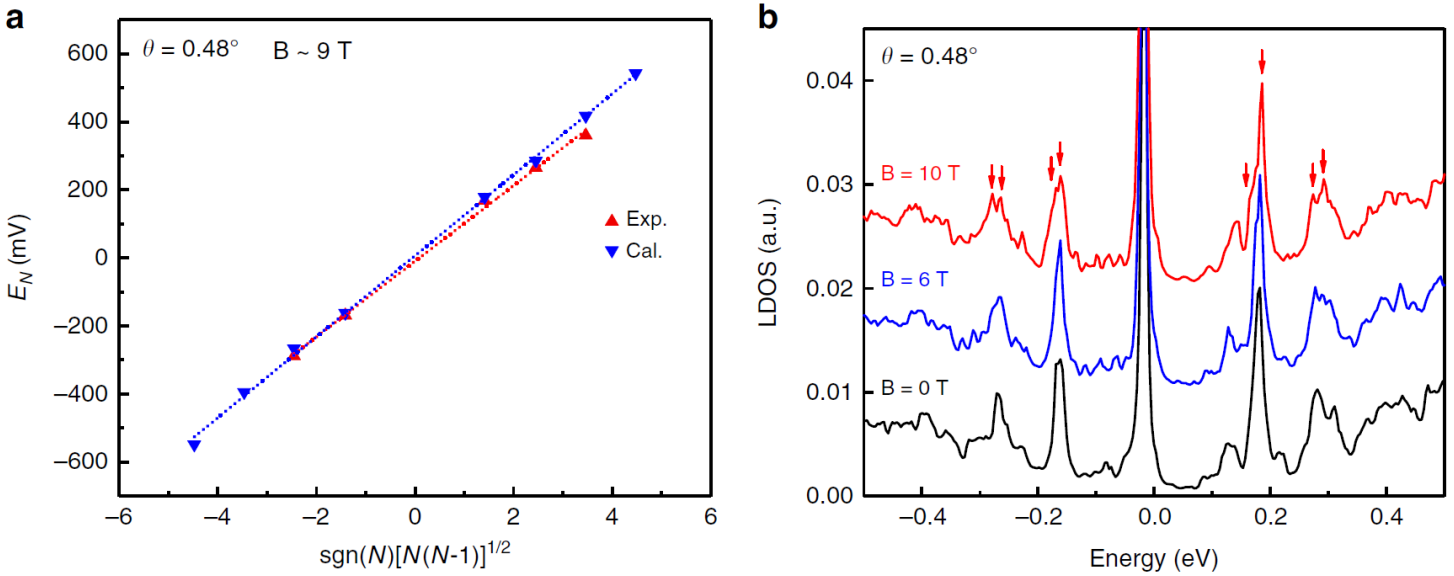

Fig. 2 Pseudo-Landau levels in the deformed twisted bilayer graphene with $\theta = 0.48°$. a Linear fit of the equation $E_N \propto \sqrt{N(N-1)}$ and the obtained pseudo magnetic fields is about 9 T. **b** Calculated LDOS at AA region under the external magnetic fields, in which we can confirm the splittings of the pseudo-Landau level due to the break of the valley degeneracy.

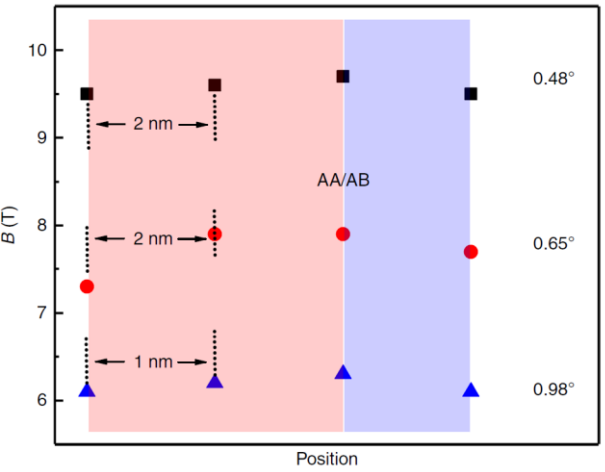

Fig. 5 The fitted pseudo-magnetic field of TBGs with different twisted angles around the region of AA/AB transtion. The obtained PMFs increase with the decreasing twisted angles and the PMF areas are distributed near the AA regions with its maximum value occuring at the AA/AB transitions, which is highly consistent with our calculated results.

Quasicrystals

Unrelaxed moire pattern is periodic if $\cos\theta = \frac{3q^2 - p^2}{3q^2 + p^2}$ with integer p and q

$\theta = 30^\circ$ incommensurate (quasicrystal) structure

Contrary to conventional 3D quasicrystals graphene quasicrystals are easily tunable!

For so large misorientation angle atomic relaxation is negligible and we are always in incommensurate phase

Dodecagonal bilayer graphene quasicrystal and its approximants

npj Computational Materials (2019)5:122

Guodong Yu[1,2,3], Zewen Wu[1,3], Zhen Zhan[1], Mikhail I. Katsnelson[2] and Shengjun Yuan[1,2*]

PHYSICAL REVIEW B **102**, 045113 (2020)

Pressure and electric field dependence of quasicrystalline electronic states in 30° twisted bilayer graphene

Guodong Yu,[1,2,*] Mikhail I. Katsnelson,[2] and Shengjun Yuan[1,2,†]

PHYSICAL REVIEW B **102**, 115123 (2020)

Electronic structure of 30° twisted double bilayer graphene

Guodong Yu,[1,2] Zewen Wu,[1] Zhen Zhan,[1] Mikhail I. Katsnelson,[2] and Shengjun Yuan[1,2,*]

Quasicrystals II

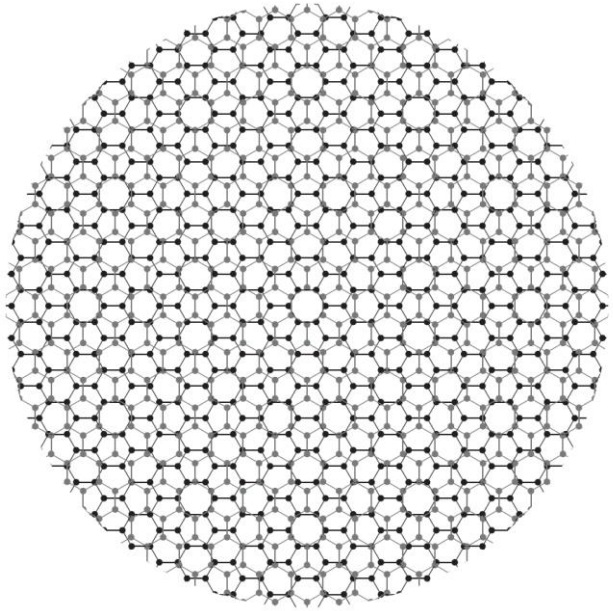

Using approximants to calculate electronic structure; elementary cell is huge but doable via tight-binding propagation method

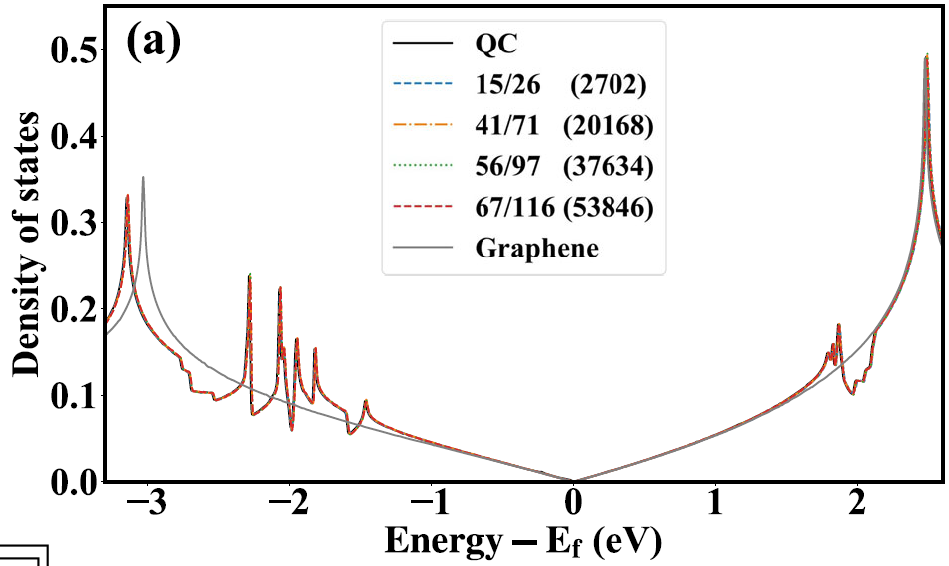

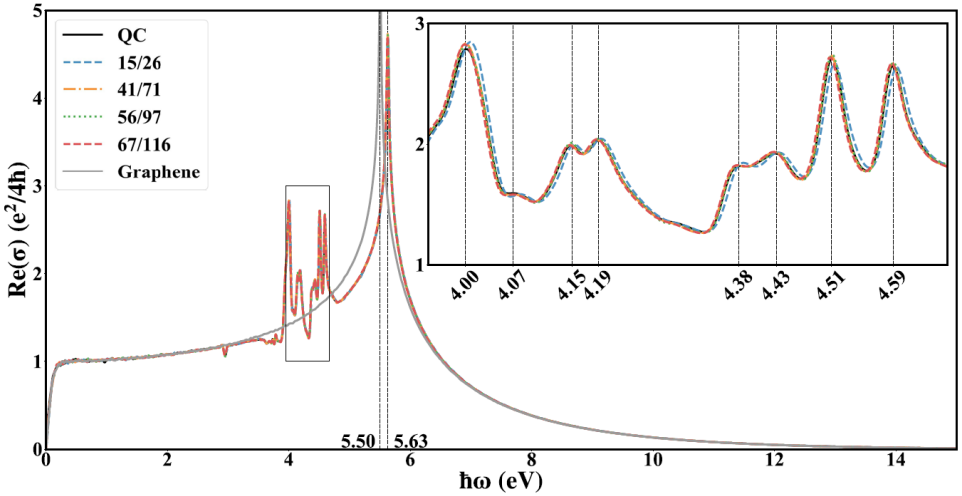

Bright features appear only far enough from the conical point

Quasicrystals III

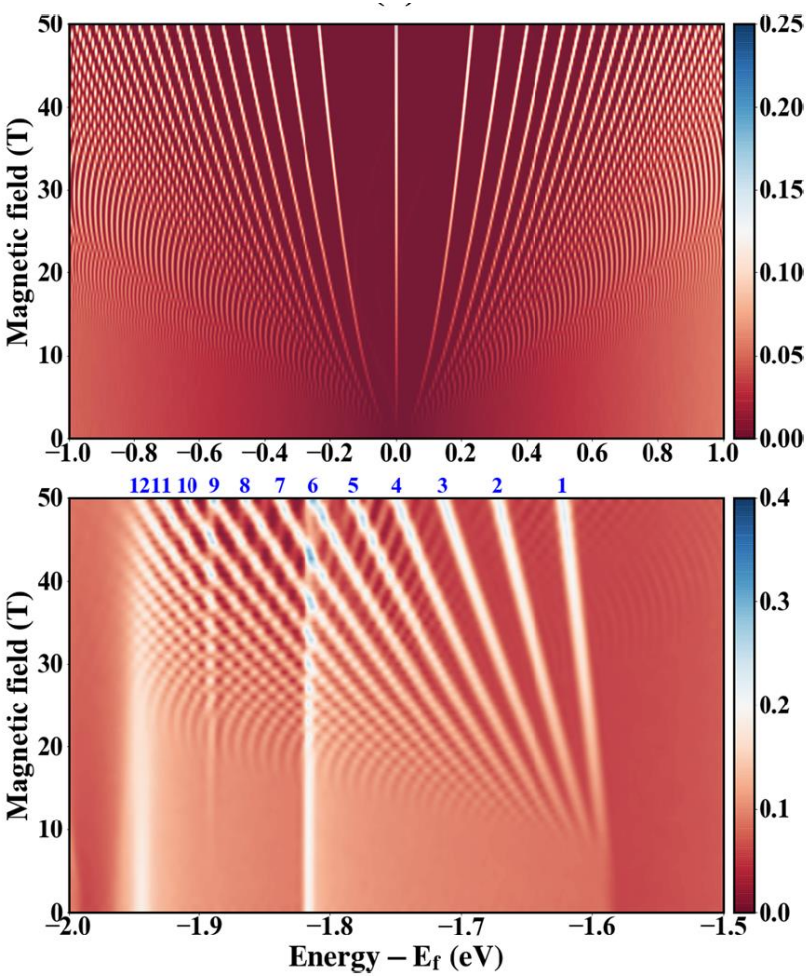

Landau levels (Hofstadter batterfly)

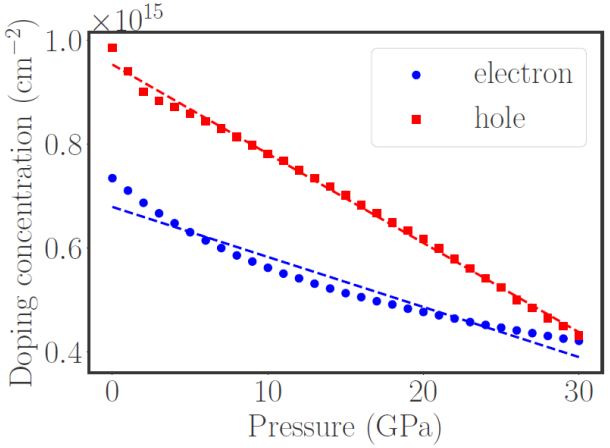

FIG. 5. The concentrations of holes and electrons that are needed to tune the Fermi level to meet the VBM and CBM.

Uniaxial pressure moves the singularities closer to the Fermi energy

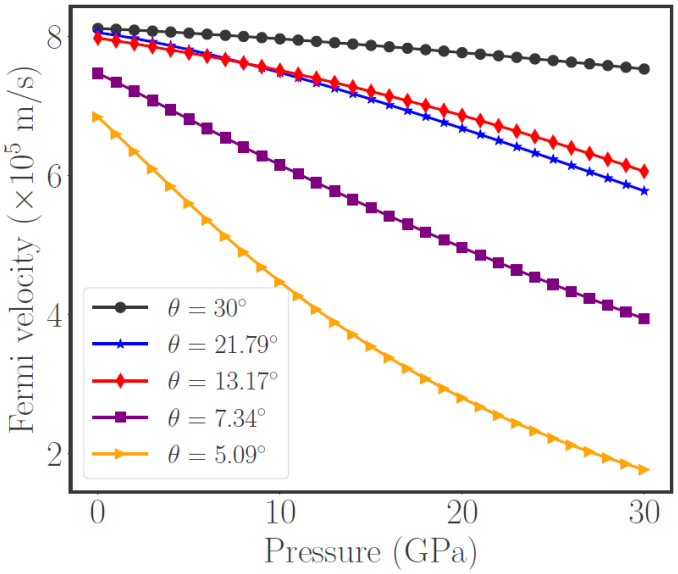

Main collaborators

Annalisa Fasolino, Merel van Wijk, Guus Slotman (Nijmegen)
Kostya Novoselov (Manchester and Singapore)
Yuri Gornostyrev (Ekaterinburg)
Evgeny Stepanov (Nijmegen and Hamburg)
Shengjun Yuan and Guodong Yu (Wuhan)

Conclusions

- Atomic relaxation is very important for small enough misorientation angles
- Twisted VdW heterostructures are model systems to study physics of commensurability and incommensurability in condensed matter
- Description in terms of vortices, dislocations and other topological effects may be very suitable
- Second-harmonic generation can be a sensitive experimental tool to study commensurate-incommensurate transition

One more story: Fermi condensate

From Standard Model of particle physics to room-temperature superconductivity

G.E. Volovik

February 11, 2021

PRL 112, 070403 (2014) PHYSICAL REVIEW LETTERS week ending 21 FEBRUARY 2014

Fermi Condensation Near van Hove Singularities Within the Hubbard Model on the Triangular Lattice

Dmitry Yudin,[1] Daniel Hirschmeier,[2] Hartmut Hafermann,[3] Olle Eriksson,[1] Alexander I. Lichtenstein,[2] and Mikhail I. Katsnelson[4,5]

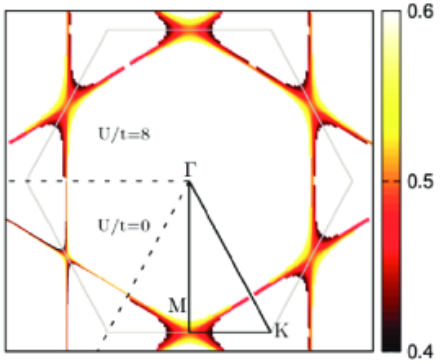

FIG. 4 (color online). Broadened Fermi surface within ±0.1 electrons for $U/t = 8$ and $T/t = 0.1$. The lower left sextant shows the noninteracting result.

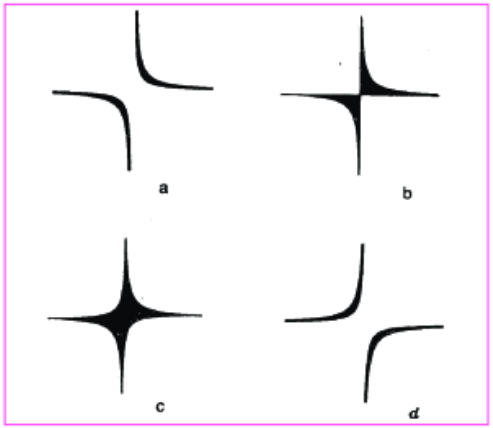

Письма в ЖЭТФ, том 59, вып.11, стр.798 - 802, ©1994 г. 10 июня

ON FERMI CONDENSATE: NEAR THE SADDLE POINT AND WITHIN THE VORTEX CORE

G.E. Volovik

Second story: Van Hove scenario and flat band formation

Example: Van Hove filling and optimal doping in high-Tc superconductors (also – pseudogap, etc.)

Irkhin, Katanin & MIK, PRB 64, 165107 (2001); PRL 89, 076401 (2002)

We consider t-t' Hubbard model on the square lattice:

$$H=\sum_{\mathbf{k}} \varepsilon_{\mathbf{k}} c^{\dagger}_{\mathbf{k}\sigma} c_{\mathbf{k}\sigma} + U\sum_{i} n_{i\uparrow} n_{i\downarrow} \qquad (1)$$

with

$$\varepsilon_{\mathbf{k}} = -2t(\cos k_x + \cos k_y) + 4t' \cos k_x \cos k_y + 4t' - \mu, \qquad (2)$$

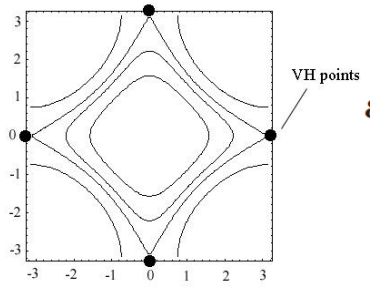

Near VHS:

$$\varepsilon^{A}_{\mathbf{k}} = -2t(\sin^2\varphi \overline{k}_x^2 - \cos^2\varphi k_y^2)$$

$$\varepsilon^{B}_{\mathbf{k}} = 2t(\cos^2\varphi k_x^2 - \sin^2\varphi \overline{k}_y^2)$$

$$2\varphi = \cos^{-1}(2t'/t)$$

When Fermi energy coincides with VHS: relevant vertices are divergent, opportunity of non-Fermi- liquid behavior (Dzialoshinskii, 1987)

Van Hove scenario and flat band formation II

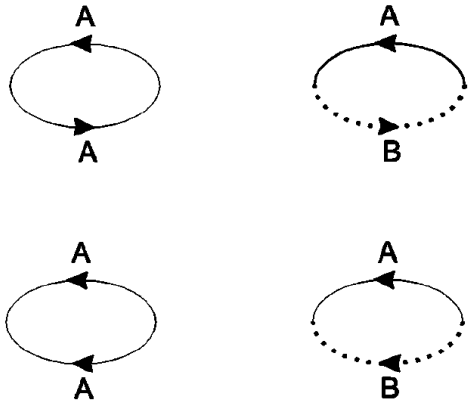

Particle-hole channel

$$\chi^{A}_{\mathbf{q}} = \sum_{\mathbf{k}} \frac{f(\varepsilon^{A}_{\mathbf{k}}) - f(\varepsilon^{A}_{\mathbf{k}+\mathbf{q}})}{\varepsilon^{A}_{\mathbf{k}} - \varepsilon^{A}_{\mathbf{k}+\mathbf{q}}} = \frac{z_0}{4\pi^2 t}(\xi_+ + \xi_-),$$

$$\chi^{AB}_{\mathbf{q}+\mathbf{Q}} = \sum_{\mathbf{k}} \frac{f(\varepsilon^{A}_{\mathbf{k}}) - f(\varepsilon^{B}_{\mathbf{k}+\mathbf{q}})}{\varepsilon^{A}_{\mathbf{k}} - \varepsilon^{B}_{\mathbf{k}+\mathbf{q}}}$$

$$= \frac{1}{2\pi^2 t}\min(z_{\mathbf{Q}}\xi_+, z_{\mathbf{Q}}\xi_-, \xi_+\xi_-).$$

$$z_0 = 1/\sqrt{1-R^2}$$

$$z_{\mathbf{Q}} = \ln[(1+\sqrt{1-R^2})/R]$$

$$R = 2t'/t$$

$\xi_{\pm}$ log divergent

Particle-particle channel

$$\Pi^{A}_{\mathbf{q}} = \sum_{\mathbf{k}} \frac{1 - f(\varepsilon^{A}_{\mathbf{k}}) - f(\varepsilon^{A}_{\mathbf{k}+\mathbf{q}})}{\varepsilon^{A}_{\mathbf{k}} + \varepsilon^{A}_{\mathbf{k}+\mathbf{q}}} = \frac{c_0}{4\pi^2 t}\xi_+\xi_-$$

$$\Pi^{AB}_{\mathbf{q}+\mathbf{Q}} = \sum_{\mathbf{k}} \frac{1 - f(\varepsilon^{A}_{\mathbf{k}}) - f(\varepsilon^{B}_{\mathbf{k}+\mathbf{q}})}{\varepsilon^{A}_{\mathbf{k}} + \varepsilon^{B}_{\mathbf{k}+\mathbf{q}}} = \frac{c_{\mathbf{Q}}}{2\pi^2 t}\min(\xi_+, \xi_-)$$

$$c_0 = 1/\sqrt{1-R^2}$$

$$c_{\mathbf{Q}} = \tan^{-1}(R/\sqrt{1-R^2})/R$$

Van Hove scenario and flat band formation III

Parquet summation of divergent diagrams (Irkhin, Katanin, MIK 2001)

Competing channels of instabilities (FM, AFM, d-wave pairing) – mutual suppression!

Phase diagram at Van Hove filling

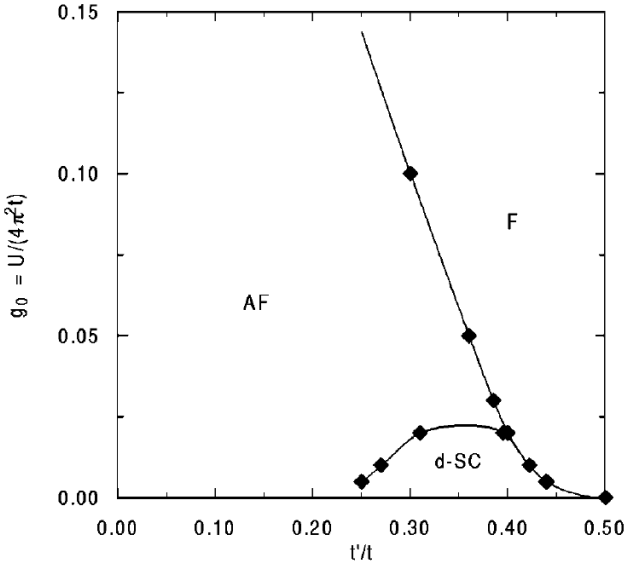

Almost exact solution for small enough *U*

Objection (P. W. Anderson): who cares on the theory working in one point?

Van Hove scenario and flat band formation IV

VOLUME 89, NUMBER 7 PHYSICAL REVIEW LETTERS 12 AUGUST 2002

Robustness of the Van Hove Scenario for High-T_c Superconductors

V. Yu. Irkhin, A. A. Katanin, and M. I. Katsnelson

If one take into account only renormalization of *dispersion*

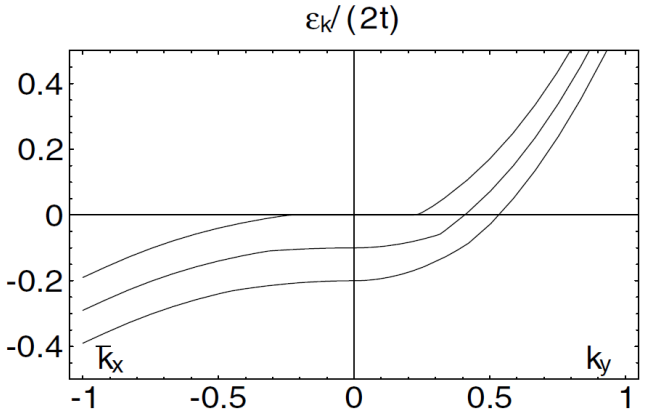

FIG. 1. Quasiparticle dispersion for $t'/t = -0.3$ and $U = 4t$ from RG approach. The values of the chemical potential are $\tilde{\mu} = 0, -0.2t, -0.4t$ (from top to bottom).

Looks like flat band formation

Perturbative RG treatment

Damping is divergent, NFL!!!
Difference with "Fermi condensation" phenomenology,
Khodel & Shaginyan (1990)

$$\delta\rho(\varepsilon) \simeq \frac{k_c^2}{\pi|\varepsilon|}\frac{C\ln(\Lambda t/|\varepsilon|)}{[1 + C\ln^2(\Lambda t/|\varepsilon|)]^2}, \qquad C = \frac{g_0^2 \ln 2}{\sin^2 2\varphi}$$

$$\tilde{\mu}(n) = \Lambda t \exp(-\text{const}/|n - n_{\text{VH}}|^{1/2})$$

Pinning Fermi energy to VHS

Triangular Lattice- VHS

PRL 112, 070403 (2014) PHYSICAL REVIEW LETTERS week ending 21 FEBRUARY 2014

Fermi Condensation Near van Hove Singularities Within the Hubbard Model on the Triangular Lattice

Dmitry Yudin,[1] Daniel Hirschmeier,[2] Hartmut Hafermann,[3] Olle Eriksson,[1]
Alexander I. Lichtenstein,[2] and Mikhail I. Katsnelson[4,5]

$$\varepsilon_{\mathbf{k}} = -2t\left(\cos k_x + 2\cos\frac{k_x}{2}\cos\frac{k_y\sqrt{3}}{2}\right) - \mu$$

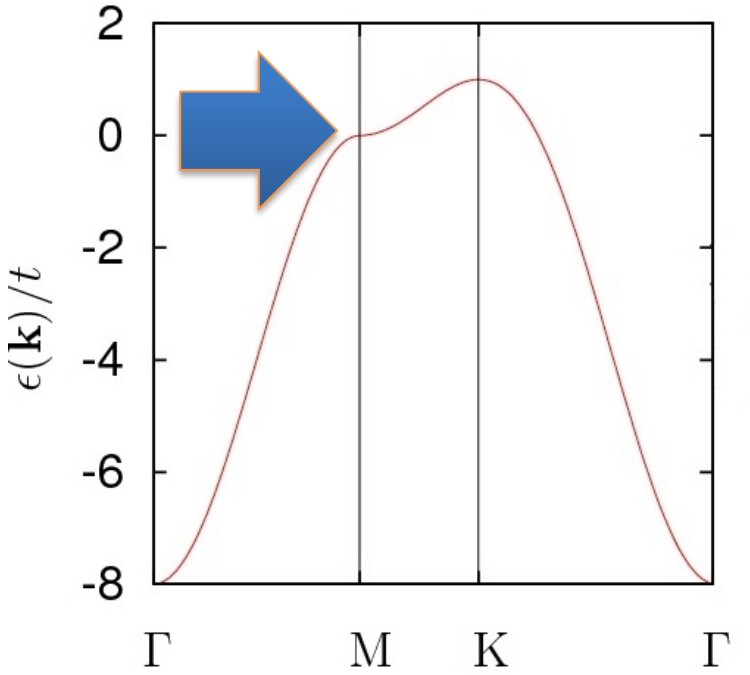

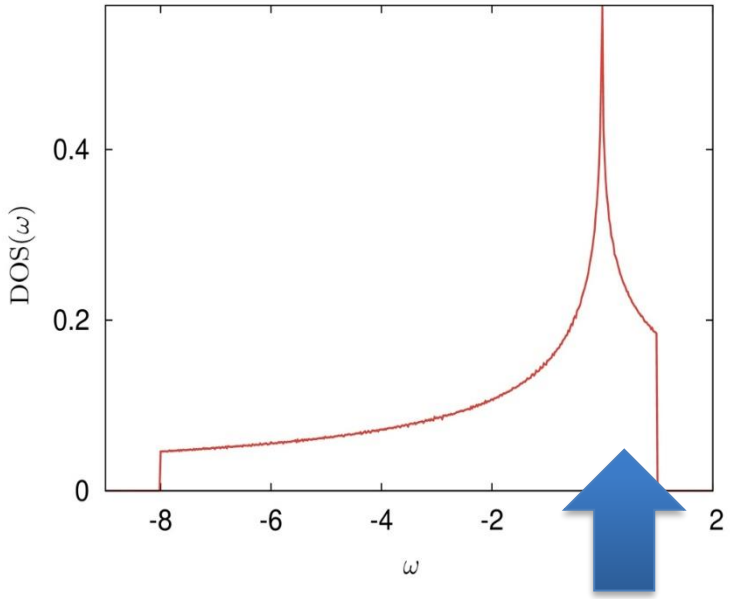

$$N(\varepsilon) = \frac{1}{\pi^2 t\sqrt{3}} K\left(\frac{1}{2} + \frac{|\varepsilon| + 2t - \varepsilon^2/4t}{4\sqrt{t\,(|\varepsilon| + t)}}\right) \sim_{|\varepsilon|/t \ll 1} N_0 \log\left(\frac{2t}{|\varepsilon|}\right)$$

$$N_0 = \sqrt{3}/(2\pi^2 t)$$

Van Hove sinqularity at filling n=2/3

Dual fermion approach

Spectral Function

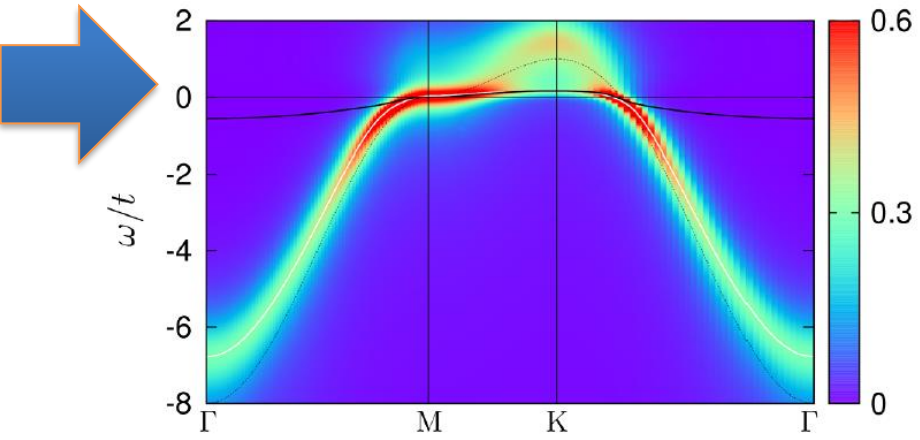

$U/t = 8$ and $T/t = 0.05$

The effect survives at relatively high temperatures, may be suitable for the observation in optical lattices

Microscopic realization of the fermion condensate

Ladder DF approx.

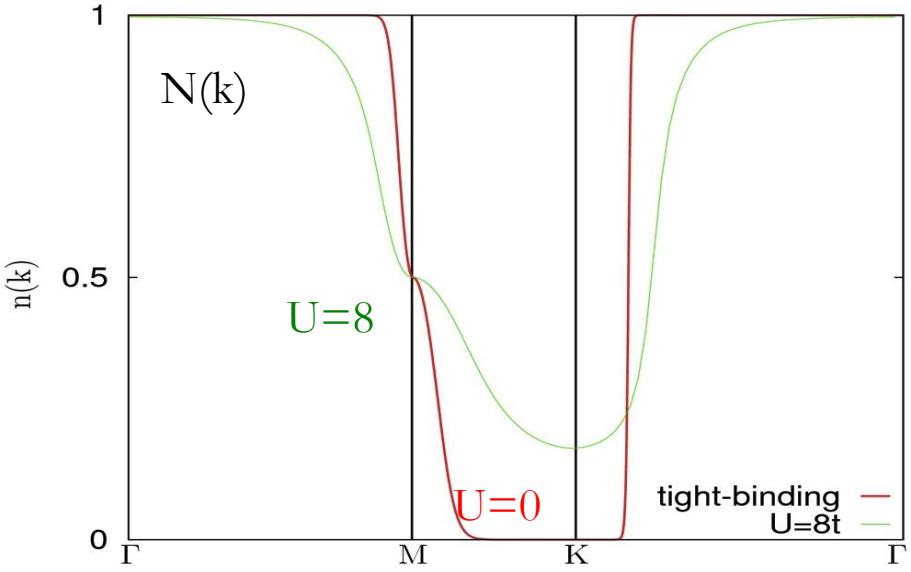

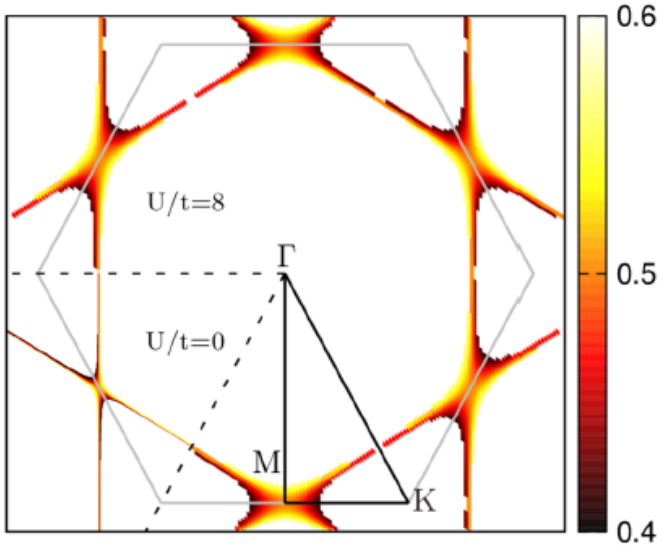

FIG. 4 (color online). Broadened Fermi surface within ±0.1 electrons for $U/t = 8$ and $T/t = 0.1$. The lower left sextant shows the noninteracting result.

Experiment?!

PHYSICAL REVIEW B **100**, 121407(R) (2019)

Rapid Communications

Introducing strong correlation effects into graphene by gadolinium intercalation

S. Link,[1] S. Forti,[1,*] A. Stöhr,[1] K. Küster,[1] M. Rösner,[2,3,4] D. Hirschmeier,[5] C. Chen,[6] J. Avila,[6] M. C. Asensio,[7] A. A. Zakharov,[8] T. O. Wehling,[2] A. I. Lichtenstein,[5] M. I. Katsnelson,[4] and U. Starke[1,†]

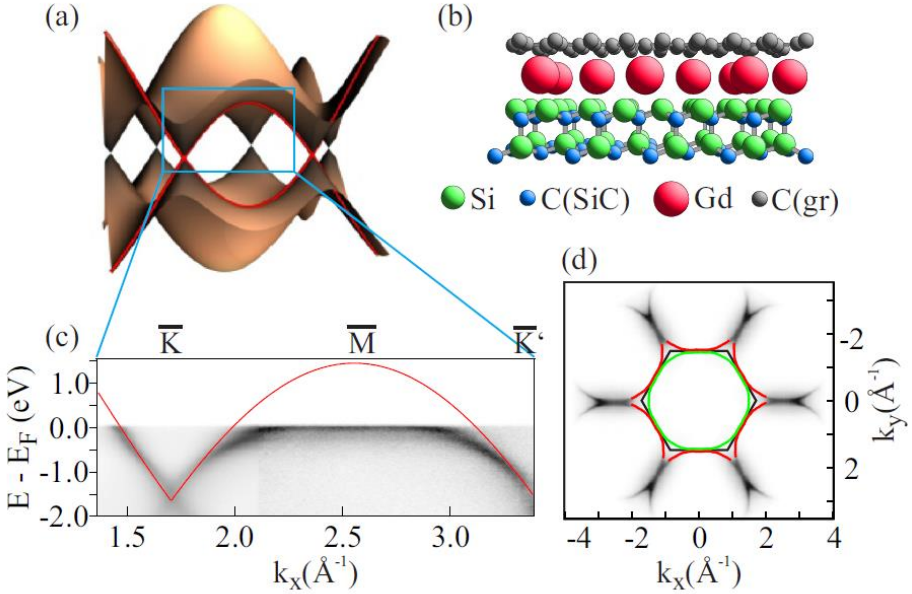

FIG. 1. ARPES on Gd-intercalated ZLG: (a) Illustration of graphene's π bands. (b) Side view model of the intercalation system. (c) Two concatenated ARPES measurements cutting from $\overline{\text{K}}$ over $\overline{\text{M}}$ to $\overline{\text{K}}'$ together with a band modeled with NN-TB (red trace). The left part (below 2.1 Å^{-1}) was taken with 30 eV and the right part (above 2.1 Å^{-1}) with 100 eV photon energy. (d) Symmetrized FS taken with 90 eV photon energy together with its experimental fit (red and green lines). The black hexagon represents graphene's first BZ.

ARPES evidence of band flattening?!

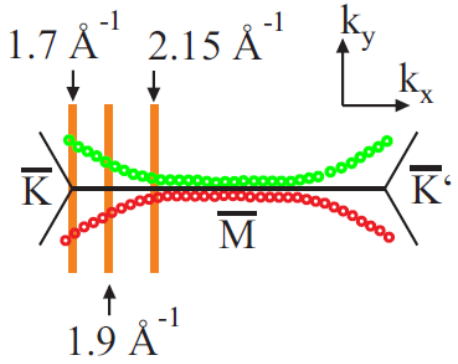

Theoretical spectral density (black)